ACS Sustainable Chemistry & Engineering

pubs.acs.org/journal/ascecg

Research Article

Green Monomers for 3D Printing: Epoxy-Methacrylate Interpenetrating Polymer Networks as a Versatile Alternative for Toughness Enhancement in Additive Manufacturing

Antonella Fantoni, Jakob Ecker, Mojtaba Ahmadi, Thomas Koch, Jürgen Stampfl, Robert Liska, and Stefan Baudis*

Cite This: *ACS Sustainable Chem. Eng.* 2023, 11, 12004−12013

Read Online

ACCESS | Metrics & More | Article Recommendations | Supporting Information

ABSTRACT: Photopolymerization represents an environmentally friendly polymerization technique due to the ability of solvent-free and room-temperature curing. However, industrially used resins are usually derived from fossil resources, inherently increasing the environmental impact of such materials. Herein, the preparation of sequential interpenetrating polymer networks (IPNs) with a high content of renewable carbon by means of free radical photopolymerization and thermal epoxy curing was investigated in detail. Therefore, poly(ethylene glycol) dimethacrylate was used as UV-curable monomers, and resorcinol diglycidyl ether and trimethylolpropane were polymerized via step-growth polyaddition. Before the fabrication of IPNs, the networks were evaluated separately regarding their reactivity by means of (photo)-differential scanning calorimetry and real-time near-infrared photorheology. A combination of both networks resulted in IPNs with superior (thermo)mechanical properties and the ability to 3D-print complex shapes via stereolithography.

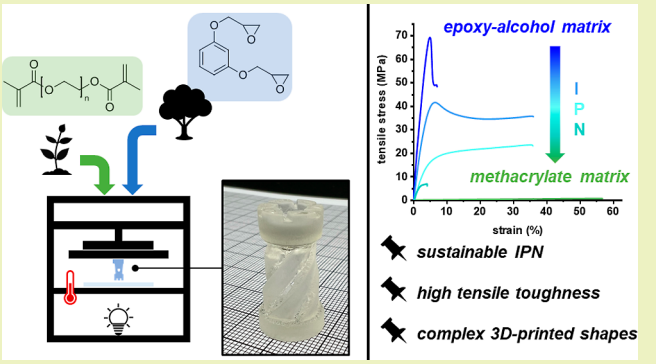

KEYWORDS: *interpenetrating polymer network, methacrylate, epoxy, dual-curing, stereolithography, bio-based monomers*

INTRODUCTION

Over the last few decades, increasing industrial and scientific research focused on sustainable alternatives to replace petroleum-based polymeric materials has been conducted. Next to the predicted scarcity of fossil resources, evermore social emphasis has shifted toward the environmental impact of such materials, as conventionally cross-linked fossil-based polymers bear a large carbon footprint and are inherently non-recyclable or (bio)degradable.[1,2]

Furthermore, research on polymeric materials has always focused on improving their properties via the implementation of unique network configurations. Interpenetrating polymer networks (IPNs) are defined as a combination of two or more polymer networks that are not covalently bonded to each other, thus showing merely physical interaction.[3] Since their discovery in 1914 by Aylsworth, different types of IPNs have been developed, comprising sequential, simultaneous, latex, gradient, or thermoplastic IPNs that are formed via different polymerization methods or use diverse initial blended components.[4] While early research focused mainly on thermal polymerization modes, photopolymerization has been proposed to produce IPNs in an environmentally friendly manner. Hybrid free radical and cationic photopolymerization of (meth)acrylate/epoxy monomers was intensively studied regarding polymerization kinetics and the resulting (thermo)mechanical properties.[5−8] Along with the investigation of photopolymerizable IPNs, IPN-resins for additive manufacturing technologies (AMT) have been developed. AMT, also known as 3D-printing or rapid prototyping, have gained significant importance due to short production times and the ability to introduce high shape complexity, design flexibility, and low material waste.[9,10] Stereolithography (SLA) represents a frequently used AMT method that utilizes a laser to cure liquid photopolymerizable monomers with high precision and layer thicknesses of up to 200 μm.[11] Conventionally, SLA resins consist of highly reactive (meth)acrylate monomers as they exhibit high photoreactivity at room temperature but suffer from polymerization shrinkage, leading to less accurate parts.[11] However, less shrinkage is exhibited when epoxy resins are photopolymerized as a result of their ring opening and thus expanding curing mechanism.[12] In order to exploit their independent advantages, various additively

Received: April 13, 2023
Revised: July 7, 2023
Published: August 1, 2023

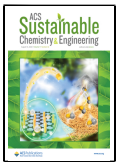

manufactured IPNs have been produced from combining (meth)acrylate and epoxy monomers.[13−15] In the last decade, research has furthermore focused on sequential dual-curing systems for AMT. Here, only one polymerization reaction is triggered by UV light, while subsequent polymerization steps are thermally or catalytically activated. Stanzione et al. developed a dimethacrylate-epoxy IPN, wherein the epoxy resin is cured using polyamines.[16] By contrast, Kuang et al. used anhydride chemistry to cure the epoxides thermally after 3D printing of a (meth)acrylate resin.[17] Furthermore, Drummer et al. proposed a dicyandiamine-based methacrylate epoxy blend system for SLA.[18]

However, the majority of photopolymerizable IPNs contain diglycidyl ether of bisphenol A (BADGE od DGEBA) as an epoxy monomer or the (meth)acrylate modification (bis-GMA), as they impart good thermal resistance and (thermo)-mechanical properties to the photopolymer networks.[7,16−18] But, bisphenol A is known to act as a reprotoxic R2 substance and was originally used as an artificial estrogen. Hence, this endocrine disruptor may lead to alterations in both the immune and reproductive systems.[19] Additionally, the high carbon footprint, volatility, and uncertainty of oil price on fossil-based monomers call for the development of sustainable resins for 3D printing. Furthermore, there is a lack of providing greener alternatives from renewable resources that give high-performance dual-cured IPNs.

In this work, we demonstrate the fabrication of sustainable IPNs via a dual-curing strategy. The matrix should be a rigid thermally curable epoxy alcohol step-growth network. For toughening and to make the resin printable by light-based AMT, a soft UV−vis curable methacrylate should be used. Therefore, we selected a photopolymerizable high-molecular-weight poly(ethylene glycol) dimethacrylate. As a reference system, a low-molecular-weight poly(ethylene glycol) (PEG) dimethacrylate (PEG750DMA, M_W ∼750 Da) was chosen. High-molecular-weight additives are known to act as toughening agents, as long polymer chains detangle under mechanical stress,[20] whereas PEG750DMA forms a tightly cross-linked network. Therefore, the influence of cross-linking density on the independent networks need to be evaluated as well as the impact on IPNs. Although the precursor PEG is typically produced from fossil resources, synthetic routes for the synthesis starting from sugar fermentation have recently been proposed.[21] Photopolymerizable motifs were integrated by modification with methacrylic end groups. Although this procedure is usually performed using dichloromethane as the solvent and triethylamine as an acid scavenger, recent studies propose the use of tetrahydrofuran as a greener solvent and enzymatic catalysis using CAL-B.[22] Furthermore, the influence of isobornyl methacrylate (IBMA) as bio-derived reactive diluents on both viscosity and mechanical properties of the polymers was investigated.[23] Interestingly, the methacrylic acid-derivative for the modification of both PEG and isoborneol can be obtained via decarboxylation of bio-based itaconic and citric acid.[24] Thereby, all the monomers for the soft network can be produced purely from renewable carbon (Figure S11a−d). Following photopolymerization to give an elastic and form-stable soft methacrylate-based network, an epoxy resin was selected as a rigidity-providing hard network. Here, resorcinol diglycidyl ether (RDGE) was chosen as renewable epoxy components due to the presence of aromatic moieties that impart rigidity and stiffness.[25] Diglycidyl ether of resorcinol is prepared from resorcinol, a *meta*-substituted di-phenol that can be obtained from biomass by the fermentation of catechins[26] or by fermentation of glucose into inositol, chemical conversion of the latter into 1,3,5-benzenetriol, and finally reduction to the diol resorcinol.[27] Diglycidyl ether has been prepared by *O*-glycidylation in good yield in the literature.[28] Aromatic polyphenols are usually converted into the epoxy derivative by direct glycidylation using epichlorohydrin in aqueous sodium hydroxide solution by the use of phase-transfer catalysts.[29] Interestingly, although epichlorohydrin is mainly produced from fossil resources, it can also be obtained from bio-based glycerol.[30] Usually epoxy resins are cured via cationic photopolymerization in AMT.[31] Although fast gelation and curing are possible, chain-growth polymerization gives inhomogeneous networks. Recently, homogenization in epoxy-based polymers was achieved by adding equimolar amounts of alcohols and altering the mechanism toward a step-growth reaction.[32] Here, sugar-derived multifunctional alcohol (trimethylolpropane) was used,[33] thus possibly making also the second network purely bio-based (Figure S11e−h). Although positive effects were observed for pure epoxy-alcohol networks, the influence of applying such resins for IPNs have to be evaluated.

Herein, (photo)reactivity and thermomechanical properties of soft and hard networks were analyzed separately by means of (photo)-differential scanning calorimetry (DSC), real-time near-infrared (RT-NIR)-photorheology, dynamic mechanical thermal analysis (DMTA), and tensile testing. For the methacrylate-based network, the influence of the PEG-spacer on elasticity and photoreactivity was evaluated. Regarding the epoxy-based network, the effect of the polymerization mode (chain-growth vs step-growth) on both reactivity and material properties were assessed. Thermomechanical properties of the combination of a high-molecular-weight methacrylate and a step-growth epoxy-alcohol network was systematically investigated and atomic force microscopy (AFM) was used to evaluate the network formation of the final hybrid material. Furthermore, the effects of introducing the higher cross-linked soft matrix and a chain-growth polymerized epoxy-based hard network into IPNs were examined. Thereby, a detailed investigation of network formation and its effects on final thermomechanical properties of IPNs was conducted. Finally, we present the first dual-curable methacrylate and epoxy-alcohol IPN concept for 3D printing using bio-based monomers.

EXPERIMENTAL SECTION

Materials and Methods. Utilized materials, synthesis, and characterization [incl. attenuated total reflection−Fourier transform infrared (ATR−FTIR) spectroscopy] can be found in the Supporting Information.

Formulation and Specimen Preparation. Formulations of the soft matrix were prepared by mixing 1 wt % of the photoinitiator (PI) Speedcure TPO-L with the corresponding monomers. The final soft matrix (S100) consisted of 20 wt % isobornylmethacrylate (IBMA), 80 wt % poly(ethylene glycol) dimethacrylate (PEG20kDMA, M_w ∼20 kDa), and additional 1 wt % of the PI. For soft matrix reference (SR100), PEG750DMA (M_w ∼750 Da) was used. Formulations were cured in silicone molds (5 × 2 × 40 mm^3 for DMTA; ISO 527 test specimen 5b for tensile tests) with a Lumamat 100 light oven (Ivoclar Vivadent AG) with 6 Osram Dulux L Blue 18 W lamps (400−580 nm) for 10 min on the top as well as the backside of the sample at an intensity of ∼60 mW cm^{-2} (determined with an Ocean Optics USB 2000+ spectrometer). Formulations of the step-growth hard matrix (H100) were prepared from RDGE and trimethylolpropane (TMP) (reactive group ratio 1:1) and 1 wt % of the catalyst imidazole. For the chain-growth reference polymer (HR100), RDGE was mixed with 1 wt % imidazole. Monomer formulations were cured in silicone molds as above at 90 °C for 18 h. For IPNs, epoxy formulations (H or HR in

https://doi.org/10.1021/acssuschemeng.3c02194
ACS Sustainable Chem. Eng. 2023, 11, 12004−12013

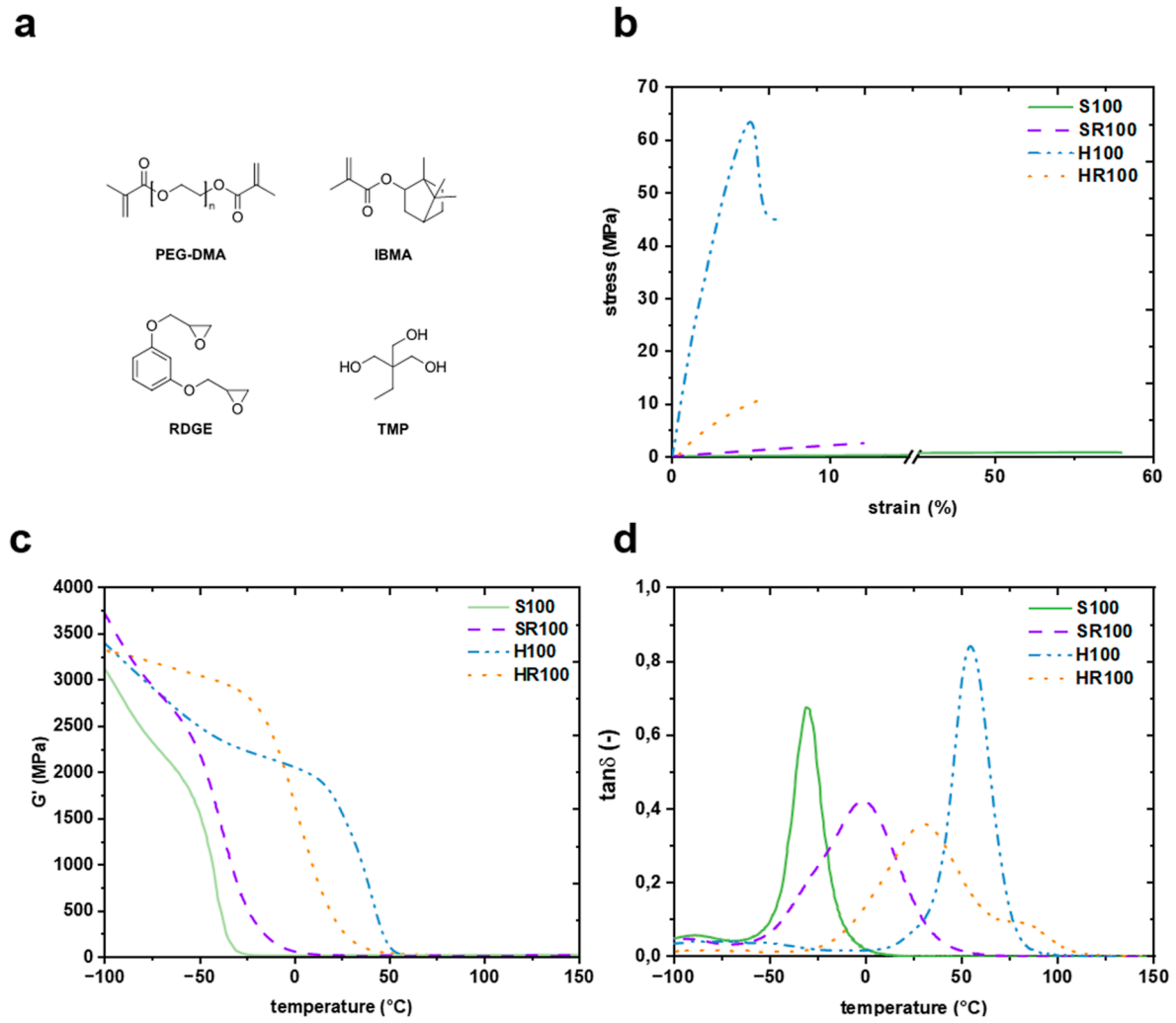

Figure 1. (a) Monomers used in this study and (b) exemplary stress−strain plot of S100, SR100, H100, and HR100. (c) Storage modulus (G') and (d) loss factor (tan δ) over temperatures for S100, SR100, H100, and HR100.

100−55 wt %) were mixed with the methacrylate monomers (S or SR in 0−45 wt %), whereby each matrix comprised 1 wt % of the respective initiator/catalyst and cured via a two-step procedure: (1) photopolymerization and (2) thermal polymerization (the same parameter as above). Cured specimens were ground to obtain uniform exact dimensions (deviations <±0.1 mm).

Real-Time Near-Infrared -Photorheology. Real-time near-infrared (RT-NIR) photorheometry was conducted on an Anton Paar MCR 302 WESP rheometer with a P-PTD 200/GL Peltier glass plate and a PP25 measuring system with a Bruker Vertex 80 FTIR spectrometer, as described previously.[34] Measurements were performed in triplicates, using ∼150 μL of monomer formulations with a constant gap size of 200 μm, a strain of 1%, and a frequency of 1 Hz. An Exfo OmniCure 2000 device with filtered light (320−500 nm) was used to irradiate samples through an optical window from underneath for 300 s at 64 mW cm^{-2} at the surface of the sample measured with an Ocean Optics USB 2000+ spectrometer. A polyethene tape (TESA 4668 MDPE) was applied on the optical window of the lower rheometer plate to facilitate sample removal. Storage (G') and loss modulus (G'') data points were obtained with 1 Hz before, 5 Hz during the first 60 s of irradiation, and 1 Hz until the irradiation period ended (4 min). Double bond conversion (DBC) was obtained by recording single spectra (at about 4 Hz) with OPUS 7.0 software by integrating the signals at a wavelength of ∼6140 cm^{-1}. DBC was determined as the ratio of peak areas at the start and at the end of the measurements.

Thermal and Thermomechanical Properties. Differential scanning calorimetry (DSC) of epoxy resins was performed on an STA 449 F1 Jupiter (Netzsch) using 10 mg (±0.1 mg) of each formulation in a sealed aluminum pan (empty pan as a reference) for temperatures between 25 and 200 °C (5 K min^{-1}). The onset of the exothermal peak (t_{onset}) was determined by intersecting tangents. Heat of reaction (ΔH) was determined through the integration of the exothermal peak. All measurements were conducted in duplicates.

Dynamic mechanical thermal analysis (DMTA) measurements were performed with an Anton Paar MCR 301 with a CTD 450 oven and an SRF12 measuring system in the torsion mode with a frequency of 1 Hz and a strain of 0.1% in a temperature range between −100 and 200 °C (2 K min^{-1}). Glass transition temperatures (T_G, maximum of the loss factor, tan δ_{max}), storage moduli at 25 °C (G'_{25}) and at the rubbery plateau (G'_r, T_G + 30 °C) were determined using the software Rheoplus/32 v3.40.

Tensile tests were performed on a Zwick Z050 tensile machine with a crosshead speed of 5 mm min^{-1} and a maximum force of 1 kN. Analysis was done with the testXpert II testing software.

AFM Measurements. Morphology investigations were performed using embedded (Struers Epo Fix Kit), ground, and polished (Struers Tegrapol 31 with SiC and diamond media, final grit size of 1 μm) polymer samples by AFM on a Park Systems XE7 AFM with an AC160TS cantilever in the tapping mode (0.7 Hz) employing Park Systems XEI 5.1.6 software.

Hot Lithography 3D Printing. The printing process was performed on a custom-build BP5 (Blue Printer 5 of TU Wien) with a digital light processing system using a transparent, rotatable, and heated material vat as previously described in detail by Stampfl et al.[35]

https://doi.org/10.1021/acssuschemeng.3c02194
ACS Sustainable Chem. Eng. 2023, 11, 12004−12013

Detailed parameters of the 3D printing can be found in the Supporting Information.

Scanning Electron Microscopy. Scanning electron microscopy (SEM) images were obtained on a Zeiss EVO 10 with a SmartSEM software and an Everhart-Thornley secondary electron detector. The acceleration voltage was set to 10 kV with a magnification of 500 times. The sample was placed on a conductive carbon pad and sputtered with a thin layer of gold to ensure conductivity.

RESULTS AND DISCUSSION

The synthesis of bio-based IPNs requires the development of orthogonally polymerizable monomers. Hence, thermally curable epoxides were chosen to form the rigidity-bearing "hard" network. For material toughening and the ability to facilitate light-based AMT, photopolymerizable high-molecular weight methacrylates served as monomers for the "soft" matrix. First, the matrices were evaluated separately before the creation and characterization of the final IPNs.

Evaluation of the Soft Matrix. Before the assessment of both photoreactivity and (thermo)mechanical properties of the soft matrix, the dimethacrylate PEG20kDMA was synthesized according to Fiore et al.[36] The conversion of the terminal hydroxyl groups into methacrylate ester bonds was confirmed via ^{31}P-NMR spectroscopy,[37] and the molecular weight (M_n ~24 kDa) was determined via gel permeation chromatography (GPC) (Tables S1−S3).

Generally, for L-AMT applications, liquid resins are required. To overcome the disadvantageous brittleness of low-molecular weight photopolymer resins, PEG20kDMA was added as a toughening agent in this study. As a result of the high molecular weight, the component appeared as a white solid with a melting point of 58 °C. Furthermore, the long polyether segments result in a low number of photoreactive units and therefore, full conversion of the double bonds is difficult to achieve in the short UV curing period. To facilitate its application as a liquid resin in SLA technologies, a reactive diluent (IBMA, Figure 1a) was added. Noteworthily, the precursor isoborneol can be derived from a pine resin, making IBMA a potential bio-based reactive diluent.[23] Adding 20 wt % of IBMA to the pristine PEG20kDMA gave a liquid resin (S100) with a sufficiently low viscosity (11 Pa s at 60 °C, Table S4). Preliminary tests furthermore proved that specimens produced from S100 give satisfactory haptic behavior for the desired applications (Table S5).

RT-NIR Photorheology. RT-NIR-photorheology is an elegant method to retrieve information about the kinetic and rheological behavior of the photopolymerization process in situ. Thereby, an assessment of potential monomers for 3D printing can be conducted. The influence of chain length and molecular weight was investigated by comparing the soft matrix formulation (S100) to a commercially available short-chain reference (SR100) (Table 1). For efficient 3D printing, a fast gelation of the respective monomers is crucial, as the time until gelation (t_g, intersection between storage G' and loss modulus G'') determines the minimum irradiation time during the 3D printing process.[34] Furthermore, NIR spectroscopy provides information about the DBC at the gel point (DBC_{gel}) and the final DBC (DBC_{final}).

Table 1. Polymerization Parameters Obtained by RT-NIR-Photorheology Measurements (Time Until Gelation t_g, Double Bond Conversion at Gel Point DBC_{gel}, Time Until 95% Conversion t_{95}, and Final Double Bond Conversion DBC_{final} of the S100 and SR100 as a Reference)[a]

	t_g (s)	DBC_{gel} (%)	t_{95} (s)	DBC_{final} (%)
S100	11.3 ± 1.7	45.8 ± 4.6	75.5 ± 3.1	91.8 ± 0.6
SR100	5.1 ± 0.4	23.1 ± 1.9	19.8 ± 0.6	95.6 ± 0.5

[a]The measurements were conducted at 60 °C.

SR100 reaches t_g after 5.1 s, much faster than S100 (11.3 s). As expected, the lower number of reactive groups, introduced by the higher molecular weight of S100 (~20 kDa), led to an increase in t_g. Additionally, the DBC at this point is nearly twice as high for S100 (46%) compared to the reference SR100 (23%) resulting from the lower cross-linking density in the first case. Following gelation, cross-linked networks are formed during further polymerization reactions. The time until reaching 95% conversion (t_{95}) and the final DBC (DBC_{final}) provide further information about the efficiency of the photopolymerization. SR100 reached t_{95} nearly four-times faster (19.8 s) than S100 (75.5 s). Interestingly, high DBC_{final} (>90%) is achieved for both formulations. Because the measurements were performed at elevated temperatures (60 °C), diffusion of propagating radicals is increased, allowing high overall DBCs. Additionally, the reactive diluent IBMA in S100 decreases the formulation's viscosity, promoting the mobility of radicals and monomers, leading to high DBCs.

(Thermo)mechanical Properties of the Soft Matrix. The viscoelastic properties of the photopolymerized specimens were determined via dynamic mechanical thermoanalysis (DMTA). The method is used to obtain the storage modulus (G') and loss modulus (G'') at different temperatures and the glass transition temperature (T_G) is determined from the maximum of the loss factor tan δ (Figure 1c,d and Table 2). A maximum of the tan δ plot of S100 was reached at −35 °C. By contrast, SR100 exhibited a higher glass transition temperature (0 °C). For both S100 and SR100, the temperature range for the glass transition was very broad, which is indicative of an inhomogeneous and nonregulated polymer network.[38] Comparing G'_r of S100 (0 °C, 15.9 MPa) and SR100 (30 °C, 16.3 MPa) demonstrates the influence of the spacer length between the methacrylate linkers (750 Da vs 20 kDa) on the cross-linking density. G' at the rubbery plateau (G'_r) describes the cross-linking density. The higher the G'_r, the higher cross-linked the underlying network.[39] Furthermore, tensile tests (Figure 1b and Table 2) revealed that S100 shows expected elastomer-like behavior, with a maximum tensile strength (σ_M) of 0.8 MPa and high elongation at break (ε_B) of 55%. Expectedly, higher cross-linking density in SR100 led to higher maximum tensile strength (2.8 MPa) and lower elongation at break (13%).

Overall, evaluation of the soft matrix highlighted that S100 showed good photoreactivity and suitable (thermo)mechanical properties. Lower T_G of S100 (−35 °C vs 0 °C for SR100) and enhanced elongation at break of 55% favor the use of S100 as an elasticity bearing soft matrix in the synthesis of IPNs.

Evaluation of the Hard Matrix. The second component of the IPN comprises the thermal polymerization of epoxy monomers with and without multifunctional alcohols. Epoxides polymerize via anionic chain-growth homopolymerization in the presence of tertiary amines. Adding equimolar amounts of alcohols leads to a variation in the polymerization mechanism that was recently published by our group. It was shown that via step-growth polyaddition of epoxy and alcohol homogeneous polymer networks, high T_G and tensile toughness were obtained.[32]

Thermal Reactivity via DSC. Thermal reactivity of the epoxide RDGE and the alcohol TMP (Figure 1a) in the

https://doi.org/10.1021/acssuschemeng.3c02194
ACS Sustainable Chem. Eng. 2023, 11, 12004−12013

Table 2. Thermomechanical Properties (G'_{25}, T_G and G'_r) and Averaged Results of Tensile Tests (σ_M, ε_B, and U_T) of IPNs[a]

	DMTA				tensile tests		
	G'_{25} (MPa)	T_G (°C)	fwhm of tan δ (°C)	G'_r (MPa)	σ_M (MPa)	ε_B (%)	U_T (MJ m^{-3})
H100	1560	54	22.6	4.58	63.7 ± 5.2	6.28 ± 0.57	2.30 ± 0.47
HR100	292	31	49.9	17.3	11.1 ± 1.30	6.62 ± 0.83	0.41 ± 0.04
S15H85	1040	52	22.8	6.08	43.7 ± 2.1	37.4 ± 5.3	12.6 ± 2.5
S30H70	997	49	23.9	2.27	23.0 ± 2.6	41.7 ± 4.2	8.12 ± 0.94
S45H55	940	47	38.4	1.87	6.11 ± 1.51	4.31 ± 1.30	0.17 ± 0.03
S100	15.8	−35	18.4	15.9	0.77 ± 0.18	54.2 ± 2.6	0.29 ± 0.13
SR100	18.1	0	50.3	16.3	2.74 ± 0.85	12.9 ± 4.5	0.20 ± 0.12
SR15H85	561.2	49	23.1	8.17	21.5 ± 0.5	29.9 ± 1.2	5.56 ± 0.32
SR51HR85	867.4	80	49.6	44.1	30.5 ± 3.9	5.8 ± 1.6	1.10 ± 0.50
S15HR85	1259	78	55.6	63.0	39.7 ± 5.0	5.0 ± 1.9	1.27 ± 0.80

[a]The hard H(R)100 and soft matrices S(R100)100 are depicted as reference.

polyaddition reaction (H100) and the anionic homopolymerization of RDGE (HR100) were studied by means of DSC. The onset temperature (87 °C) and peak temperature (104 °C) were approximately 10 °C higher for H100 compared to HR100 (75 and 94 °C, respectively). High monomer conversions (>90%) for both polymers were obtained according to FT-IR (Table S7). By comparing ΔH and the determined epoxy group conversion, the theoretical heat of polymerization ($\Delta H_{p,0}$) was calculated. $\Delta H_{p,0}$, for the polyaddition (H100), was calculated to be 97 kJ (mol epoxy)$^{-1}$, which is in good agreement with the literature-reported value of 98−111 kJ (mol epoxy)$^{-1}$ for epoxy-amine step-growth polymerizations.[40,41] By comparison, $\Delta H_{p,0}$ for the anionic homopolymerization of HR100 (100 kJ per epoxy functionality) was slightly higher than the reported heat (92 kJ per mol epoxy) for the tertiary amine-initiated anionic homopolymerization of epoxy resins.[42−44]

(Thermo)mechanical Properties of the Hard Matrix. H100 exhibited a sharp maximum of the loss factor at 54 °C (fwhm 22.6 °C), while T_G of HR100 was decreased to 31 °C. Significant broadening of the tan δ peak for HR100 (fwhm 49.9 °C) indicates inhomogeneous and unregulated polymers.[38] As previously reported by our group, polyaddition of epoxy and alcohol monomers (H100) leads to the formation of more homogeneous networks via a step-growth polymerization.[32] Furthermore, G'_{25} of H100 (1560 MPa) is significantly higher than G'_{25} of HR100 (292 MPa), which was expected due to a lower T_G (31 °C) of HR100. When comparing G'_r, somewhat higher values were obtained for HR100 (65 °C, 17 MPa) compared to H100 (85 °C, 4.6 MPa), as the underlying chain-growth polymerization led to the formation of highly cross-linked and brittle networks (Figure 1c,d and Table 2).[39]

The influences of the cross-linking density and homogeneity of different polymerization mechanisms were investigated via tensile testing (Figure 1b and Table 2). Step-growth polyaddition (H100) resulted in polymers with high tensile strength (64 MPa) and ε_B of 7%. Furthermore, a distinct yield point was exhibited by the material. By comparison, anionic homopolymerization (HR100) led to a significant decrease in σ_M (11 MPa), while ε_B remained comparable with ∼7%. Tensile tests were performed at room temperature and considering that HR100 displayed a T_G of 31 °C, a transition toward a more elastomer-like material was expected. Moreover, by integration of the tensile stress−strain plots, tensile toughness (U_T) was obtained: H100 showed a nearly six times higher U_T (2.3 MJ m^{-3}) compared to the reference HR100 (0.4 MJ m^{-3}). Thus, network homogenization and a decrease in the cross-linking density as characterized via DMTA led to toughened polymer networks.

With regard to the preparation of IPNs, the step-growth polyaddition (H100) appears to be better suited, as more homogeneous polymer networks are obtained. Furthermore, the epoxy-alcohol reaction resulted in polymers with higher tensile strength and higher T_G, that ultimately comply better with the requirements for the hard matrix, therefore they were chosen as a rigid matrix for the IPNs.

Evaluation of IPNs. After the evaluation of each independent network, the combination of soft and hard matrix was tested regarding their performance as dual curable IPNs. Mixtures of different compositions were tested and termed H(R)*x*S(R)*y*, where *x* and *y* indicate weight percentages of the hard matrix H100 or the reference HR100 and the soft matrix S100 or the reference SR100, respectively. In a preliminary study (Supporting Information Figures S5, S6 and Table S8), it was demonstrated that the polymerization mechanisms are independent from each other and co-polymerization between the networks is excluded. Furthermore, kinetics of both photopolymerization and polyaddition were compared (Figure S7), demonstrating that the final conversion of the double bonds in the soft matrix is achieved before any significant conversion is accomplished via polyaddition.

(Thermo)mechanical Properties of IPNs. To investigate the influence of adding an elastic network (S100, in various compositions from 15 to 45 wt %) to the neat stiff epoxy-alcohol network H100, DMTA and tensile tests of the resulting IPNs were performed. Before conducting (thermo)mechanical tests, conversion of the reactive groups of polymer specimens was investigated by means of ATR−IR spectroscopy. With the disappearance of the epoxy group vibration (∼910 cm^{-1}) and C═C stretching vibration (1716 cm^{-1}), high conversions (>90%) for both networks were achieved that are comparable to the conversions of each independent network. It is noteworthy to mention that all (thermo)mechanical tests were conducted with bulk-cured IPNs. However, comparing bulk-cured and 3D-printed specimens regarding their (thermo)mechanical behavior would go beyond the scope of this present study.

At first, viscoelastic properties of the IPNs were evaluated using DMTA (Figure 2a,b and Table 2).

As expected, the neat epoxy-based network (H100) exhibited the highest T_G (54 °C) and storage modulus at 25 °C (G'_{25}: 1560 MPa). Furthermore, the lowest T_G (−35 °C) and G'_{25} (15.8 MPa) were displayed by the pure elastic methacrylate network (S100). Adding 15−45 wt % of soft matrix to H100 led to a marginal decrease in T_G (S15H85: 52 °C, S30H70: 49 °C,

https://doi.org/10.1021/acssuschemeng.3c02194
ACS Sustainable Chem. Eng. 2023, 11, 12004−12013

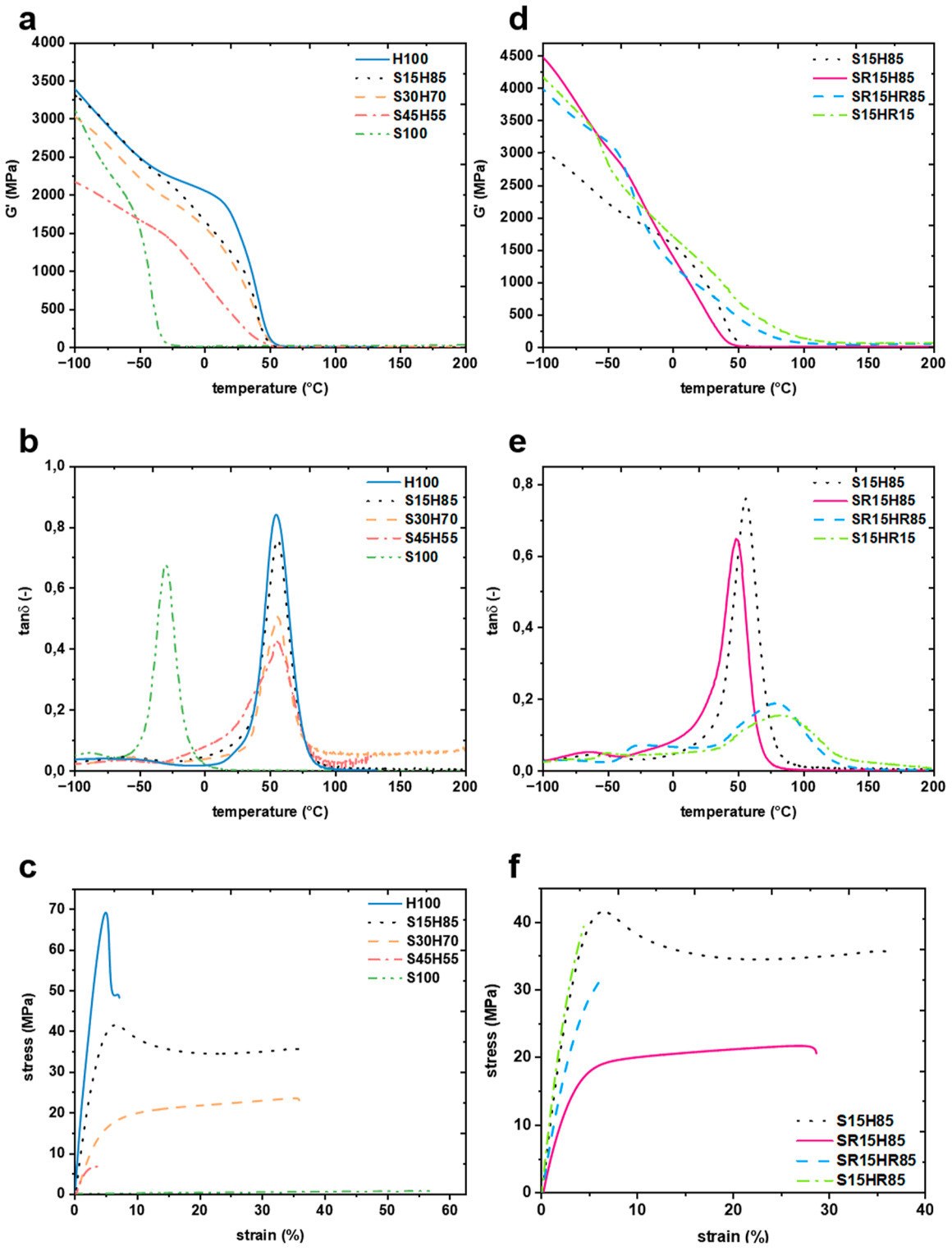

Figure 2. (a) Storage modulus (G') and (b) loss factor (tan δ) over temperature for IPNs S15H85, S30H70, and S45H55. The independent networks S100 and H100 are depicted as references. (c) Representative stress−strain curves of IPNs S15H85, S30H70, and S45H55. The independent networks S100 and H100 are depicted as references. (d) Storage moduli (G') and (e) loss factor (tan δ) over temperature of IPNs containing 85 wt % epoxy monomers and 15 wt % methacrylate monomers: S15H85, SR15H85, SR15HR85, and S15HR85. (f) Representative stress−strain curves of IPNs S15H85, SR15H85, SR15HR85, and S15HR85.

and S45H55: 47 °C). Therefore, an increase in the molecular distance between the connections in the methacrylate and epoxy network did not have a significant impact on T_G. However, as a result of adding the wide-meshed soft network, G'_{25} was lowered (S15H85: 1040 MPa, S30H70: 997 MPa, and S45H55: 940 MPa) compared to H100. Additionally, the width of the tan δ peak is associated with the homogeneity of a polymer network. Broader peaks indicate heterogeneous networks with a wide distribution of relaxation modes.[38,45] IPNs with up to 30 wt % of soft network are characterized by narrow tan δ_{max}, whereby the

https://doi.org/10.1021/acssuschemeng.3c02194
ACS Sustainable Chem. Eng. 2023, 11, 12004−12013

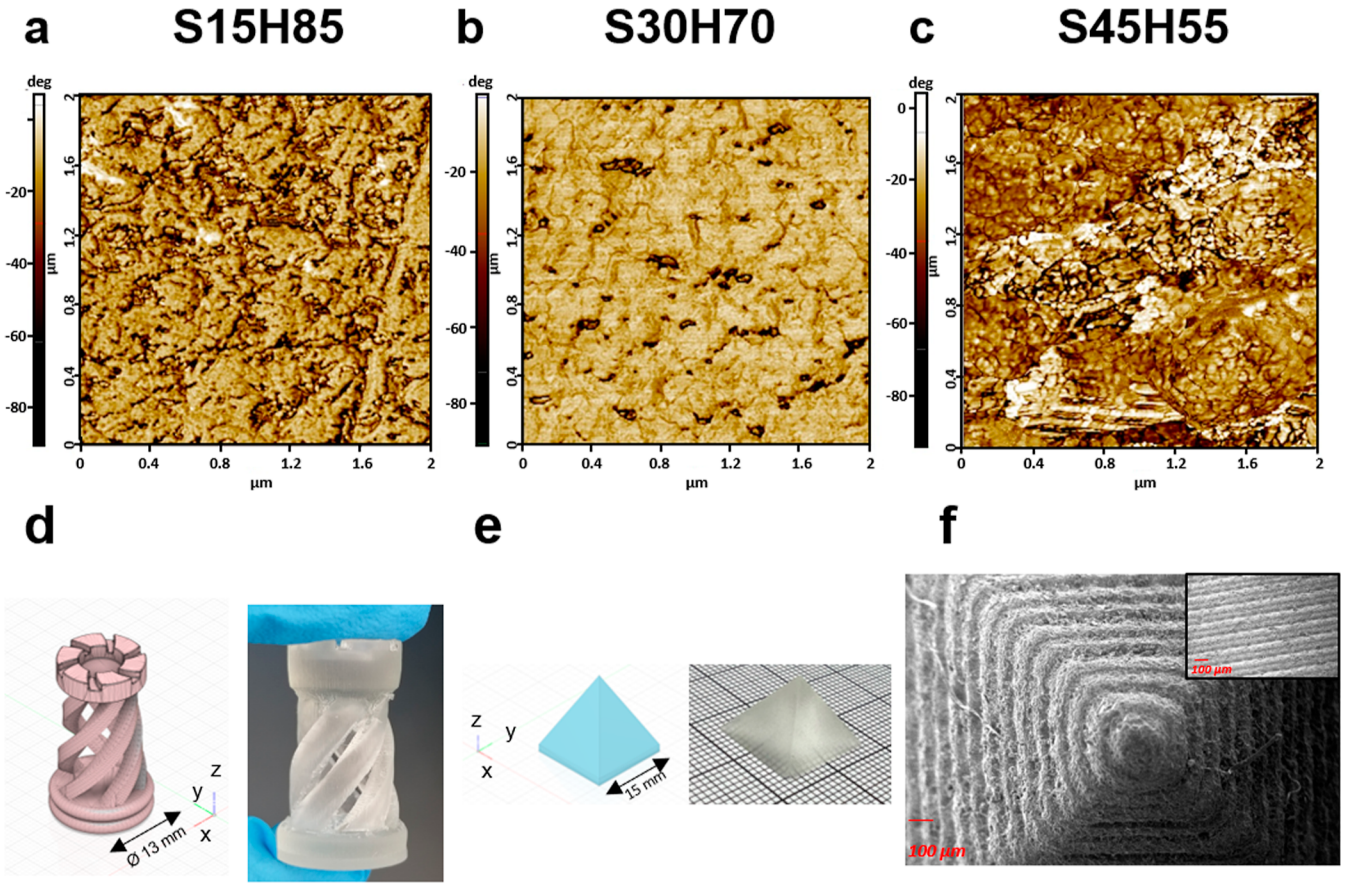

Figure 3. AFM images of IPNs containing (a) 15 wt % (S15H85), (b) 30 wt % (S30H70), and (c) 45 wt % (S45H55) methacrylate network. The soft methacrylate matrix is dispersed with a bright contrast and the epoxy phase is the continuous majority dark phase. Samples were prepared by photopolymerization of the soft matrix (S100) and subsequent thermal polymerization of the epoxy-alcohol-based hard network H100 (d) 3D-printed hollow chess tower and the corresponding CAD file, (e) 3D-printed pyramid and the corresponding CAD file, and (f) SEM image in top view of the 3D printed pyramid. Additionally, the SEM image of the side view is presented for better estimation of a layer thickness of 100 μm.

fwhm of S15H85 (22.8 °C) and S30H70 (23.9 °C) are comparable with H100 (22.6 °C). Interestingly, S45H55 displayed a strong tan δ peak broadening (fwhm: 38.4 °C), emphasizing increased heterogeneity of the networks. An explanation for this phenomenon can be found when looking at the evolution of morphology during IPN synthesis. In the first stages of polymerization, two independent networks are formed, leading to phase separation. Depending on the size of the generated domains, different properties of the final IPN are obtained. While large domains lead to the formation of broadened or multiple T_Gs, smaller domains show inward shifted T_Gs as a result of homogeneously blended networks at the molecular scale.[46]

To explore the phase distribution and surface morphologies of IPNs, AFM in the tapping mode was used. AFM in the tapping mode enables the cantilever tip to oscillate at a constant frequency. Depending on the inherent local properties of each phase, adhesion behavior will cause lower or higher delays in the cantilever-tip oscillation that are represented with variations in the phase angle.[47] While negative degree angles are caused by less adhesive hard domains, softer, and thus more adhesive, domains give positive degree angles. Figure 3 shows the phase morphology of (a) S15H85, (b) S30H70, and (c) S45H55. For systems containing 15−30 wt % of the methacrylate network (S15H85 and S30H70, respectively), homogeneous surfaces were observed. For the same systems, a single narrow tan δ peak was detected in DMTA measurements, indicating good interpenetration and compatibility of both networks (Figure 3b).[8,48] By contrast, significant tan δ peak broadening was observed for S45H55 (45 wt % methacrylate network), indicating the formation of more heterogeneous materials.[45] Indeed, in the AFM images (Figure 3c) distinct bright regions can be seen, which correspond to the softer methacrylate network. Furthermore, darker domains comprising the stiffer epoxy network are visible and the intermediate color could indicate interphases containing different ratios of both networks. Consequently, the final IPN becomes heterogeneous represented by an intermediate behavior between clear phase separation and homogeneity[49] that accounts for the abrupt deterioration of (thermo)mechanical properties of S45H55.

Furthermore, tensile tests were conducted to determine the effects of IPNs on the resulting mechanical properties (Figure 2c and Table 2). As expected, the pure epoxy-based matrix (H100) exhibited the highest σ_M (64 MPa) and a low ε_B (~6%), resulting in a tensile toughness of 1.3 MJ/m^3. The addition of high-molecular-weight additives is known to enhance the tensile toughness of the resulting materials.[50] Generally, toughness indicates the amount of deformation energy absorbed by a material before the initiated stress leads to a crack formation.[51,52] Adding 15 wt % of the methacrylate matrix (S15H85) led to a 10 times higher tensile toughness (13 MJ/m^3) while the maximum stress at break was only lowered by 30% to 44 MPa. The addition of the 2-fold amount of soft network (S30H70) lowered σ_M to 23 MPa (36% of H100), whereby ε_B

https://doi.org/10.1021/acssuschemeng.3c02194
ACS Sustainable Chem. Eng. 2023, 11, 12004−12013

increased to 42% and U_T was diminished to 8 MJ m^{-3}. Hence, the presence of high-molecular-weight PEG20kDMA in the IPNs enables detangling of the polymer chains under mechanical stress that can be seen in an increase of elongation at break. Interestingly, S45H55 displayed significantly poorer mechanical properties (σ_M: 6 MPa, ε_B: 4%, U_T: 0.2 MJ m^{-3}). These findings correlate with the increased network heterogeneity demonstrated by DMTA and AFM measurements.

Influence of Polymerization Mechanisms and Cross-Linking Density on (Thermo)mechanical Properties. In (thermo)mechanical studies, adding 15 wt % of S100 to H100 proved to be the best-performing hybrid material in both DMTA and tensile tests. Introducing a high-molecular-weight methacrylate into the rigid epoxy-based material led to the formation of materials of high tensile strength and toughness, without forfeiting the T_G of the material. To study the influence of chain length and thus cross-linking density of the PEG-backbone in IPNs, the soft matrix was substituted with SR100. Additionally, the effect of the polymerization mode of the epoxy network was investigated by the substitution of H100 with HR100 (Figure 2d,e and Table 2). High conversion of the reactive groups of each network (>90%) was determined by means of ATR−IR spectroscopy and is comparable to the independent networks.

The hard network in S15H85 and SR15H85 was synthesized via epoxy-alcohol polyaddition and resulted in narrow tan δ_{max} (fwhm of 23 °C), stemming from the homogeneous networks of the step-growth reaction.[32] Additionally, similar glass transition temperatures of around 50 °C were determined. Interestingly, via chain-growth polymerization (SR15HR85 and S15HR85), heterogeneous networks were obtained resulting in broadening of tan δ_{max} (fwhm >49 °C). The influences of the cross-linking density and network homogeneity on thermomechanical properties are obvious, if one compares S15H85 and S15HR85, which both contain the same methacrylate-based networks and differ only in the polymerization mode of the epoxy monomers. G'_r of S15HR85 (108 °C, 63 MPa) is 10 times higher than S15H85 (85 °C, 6.1 MPa), indicating highly cross-linked networks.[39] The same trend is evident for SR15H85 and SR15HR85. Polyaddition of the epoxy monomers in SR15H85 enables the formation of less cross-linked networks (89 °C, G'_r of 8 MPa), whereby homopolymerization (SR15HR85) leads to a higher degree of cross-linking and a 5-fold increase in G'_r (110 °C, 44 MPa). Interestingly, the unregulated nature of the chain growth polymerization resulted in materials of higher T_G (80 °C for SR15HR85 and 78 °C for S15HR85).

Finally, tensile tests were conducted (Figure 2f and Table 2). The effect of introducing high-molecular-weight dimethacrylate (PEG20kDMA) as a soft matrix on the mechanical properties can clearly be seen by comparison of S15H85 and SR15H85. S15H85 displayed the highest ε_B (37%) and σ_M (44 MPa) of all tested materials, resulting in an outstanding tensile toughness of 13 MJ m^{-3}. By substitution of S100 with SR100 in IPN SR15H85, ε_B was lowered to 30%, while σ_M decreased by a factor of 0.5 (22 MPa), leading to a diminished U_T of 5.6 MJ m^{-3}. Hence, tensile tests confirmed the superior influence of PEG20kDMA as a photopolymerizable precursor. Furthermore, using HR100 resulted in materials of high tensile strength (31 MPa for SR15HR85 and 40 MPa for HS15SR85), but the high degree of cross-linking of the epoxy network diminished the elongation at break of IPNs (<6%). Additionally, tensile toughness was reduced to 1.1 (SR15HR85) and 1.3 MJ m^{-3} (S15HR85), respectively. Thereby, it was shown that the combination of epoxy-alcohol polyaddition and the use of PEG20kDMA gives the best material properties that were confirmed by both DMTA and tensile tests.

Hot Lithography 3D Printing. After the assessment of (thermo)mechanical properties and phase analysis of bio-based IPNs, their applicability in hot-lithography 3D printing was tested. At first, rheology measurements (Figure S9 and Table S9) proved that IPNs containing 15−45 wt % of the soft matrix (S100) in the hard matrix (H100) exhibit a viscosity of <5 Pa s and are, therefore, applicable for the desired hot lithography technique.[53] For AMTs, it is necessary to obtain form-stable specimens before subjecting the 3D-printed objects to post-curing procedures. Figure S8 highlights that S45H55 exhibited the best form stability after photopolymerization. Therefore, complex shapes were printed from this formulation in order to prove the possibility of 3D printing of such resins. Indeed, one advantage of SLA is the fabrication of complex shapes with good final properties and good accuracy with respect to the used CAD file. To ensure high photoreactivity and low viscosity of the resin, the printing was attempted at 60 °C. Unfortunately, the high temperatures led to poor attachment of the printed layers on the building platform. Therefore, the temperature was lowered to 50 °C, which significantly improved the attachment of the polymerized parts, without sacrificing the resin's photoreactivity. As only the methacrylate matrix was cured during 3D printing, the printed objects were thermally post-cured at 90 °C for 18 h to ensure cross-linking of the epoxy network. With this setup, high accuracy with respect to the CAD files was achieved and SEM images (Figure 3d−f) confirm the high resolution of the 3D-printed pyramid. The printed layers can clearly be observed and correspond with a layer thickness of 100 μm. Moreover, good interlaminar attachment was observed. A more complex, self-standing, and hollow chess tower was produced to finally demonstrate the advantages of 3D printing compared to conventional manufacturing technologies. By the addition of 0.01 wt % of the absorber Sudan Orange, more delicate structures, such as a hollow pyramid (Figure S10b) and a hollow chess tower (Figure S10c), were fabricated (layer thickness of 100 μm).

CONCLUSIONS

Traditionally, dual curing of epoxy-methacrylate systems is performed by using fossil-based monomers, frequently containing bisphenol-A derivatives, such as BADGE or bis-GMA. Apart from their high carbon footprint, reprotoxic activity may have a negative impact on both human health and the environment. In this study, IPNs from renewable resources were synthesized via a dual-curing technique that comprised the photopolymerization of poly(ethylene glycol) dimethacrylates (M_n 750−20 kDa) as a bio-based soft matrix followed by a thermally catalyzed epoxy-alcohol polyaddition of RDGE and TMP to give the bio-based hard matrix. Investigations of the independent networks demonstrated high (photo)reactivity and conversion of both phases. This study elucidates the importance of using high-molecular-weight methacrylates as elasticity-providing monomers and epoxy-alcohol polyaddition for the subsequent thermal curing. A significant improvement of tensile toughness (up to 13 MJ m^{-3}) was achieved for IPNs containing 15 and 30 wt % of PEG20kDMA, while maintaining a T_G >45 °C. By lowering the molecular weight of the methacrylate compound to 750 Da, higher cross-linking densities and thus stiffer soft matrices were obtained, leading to a decrease in tensile toughness by 50% (5.5 MJ m^{-3}). By applying chain growth of the epoxides, the tensile toughness was even more drastically decreased (1 MJ m^{-3}).

https://doi.org/10.1021/acssuschemeng.3c02194
ACS Sustainable Chem. Eng. 2023, 11, 12004−12013

Thereby, (thermo)mechanical properties were linked with cross-linking density and mode of polymerization. Finally, complex and self-standing shapes with high resolutions were produced via SLA. Thereby, this work expands the exploitation of bio-based monomers for 3D-printing technologies.

■ ASSOCIATED CONTENT

Supporting Information

The Supporting Information is available free of charge at https://pubs.acs.org/doi/10.1021/acssuschemeng.3c02194.

Experimental details, materials and methods, including OH-value determination via ^{31}P-NMR, GPC, photo-DSC, rheology, and ATR−IR (PDF)

■ AUTHOR INFORMATION

Corresponding Author

Stefan Baudis − *Christian Doppler Laboratory for Advanced Polymers for Biomaterials and 3D Printing, Vienna 1060, Austria; Institute of Applied Synthetic Chemistry, Technische Universität Wien, Vienna 1060, Austria;* orcid.org/0000-0002-5390-0761; Email: stefan.baudis@tuwien.ac.at

Authors

Antonella Fantoni − *Christian Doppler Laboratory for Advanced Polymers for Biomaterials and 3D Printing, Vienna 1060, Austria; Institute of Applied Synthetic Chemistry, Technische Universität Wien, Vienna 1060, Austria*

Jakob Ecker − *Institute of Materials Science and Technology, Technische Universität Wien, Vienna 1060, Austria*

Mojtaba Ahmadi − *Institute of Materials Science and Technology, Technische Universität Wien, Vienna 1060, Austria*

Thomas Koch − *Institute of Materials Science and Technology, Technische Universität Wien, Vienna 1060, Austria*

Jürgen Stampfl − *Christian Doppler Laboratory for Advanced Polymers for Biomaterials and 3D Printing, Vienna 1060, Austria; Institute of Materials Science and Technology, Technische Universität Wien, Vienna 1060, Austria;* orcid.org/0000-0002-3626-5647

Robert Liska − *Institute of Applied Synthetic Chemistry, Technische Universität Wien, Vienna 1060, Austria*

Complete contact information is available at: https://pubs.acs.org/10.1021/acssuschemeng.3c02194

Notes

The authors declare no competing financial interest.

■ ACKNOWLEDGMENTS

Funding by the Christian Doppler Research Association within the framework of the "Christian Doppler Laboratory for Advanced Polymers for Biomaterials and 3D Printing" and the financial support by the Austrian Federal Ministry for Digital and Economic Affairs and the National foundation for Research, Technology, and Development are gratefully acknowledged. The authors acknowledge TU Wien Bibliothek for financial support through its Open Access Funding Program. M.A. acknowledges the funding by TU Wien's DigiPhot project.

■ REFERENCES

(1) Gandini, A. The irruption of polymers from renewable resources on the scene of macromolecular science and technology. *Green Chem.* **2011**, *13*, 1061−1083.

(2) Voet, V. S. D.; Guit, J.; Loos, K. Sustainable Photopolymers in 3D Printing: A Review on Biobased, Biodegradable, and Recyclable Alternatives. *Macromol. Rapid Commun.* **2020**, *42*, 2000475.

(3) Sperling, L. H. *Interpenetrating Polymer Networks: An Overview*; American Chemical Society, 1994; Vol. *239*, pp 3−38.

(4) Sperling, L. H. *Interpenetrating Polymer Networks and Related Materials*; Springer US, 2012.

(5) Decker, C.; Decker, D. Photoinitiated Polymerization of Vinyl Ether and Acrylate Monomer Mixtures. *J. Macromol. Sci., Part A: Pure Appl.Chem.* **1997**, *34*, 605−625.

(6) Sangermano, M.; Carbonaro, W.; Malucelli, G.; Priola, A. UV-Cured Interpenetrating Acrylic-Epoxy Polymer Networks: Preparation and Characterization. *Macromol. Mater. Eng.* **2008**, *293*, 515−520.

(7) Lecamp, L.; Pavillon, C.; Lebaudy, P.; Bunel, C. Influence of temperature and nature of photoinitiator on the formation kinetics of an interpenetrating network photocured from an epoxide/methacrylate system. *Eur. Polym. J.* **2005**, *41*, 169−176.

(8) Rocco, C.; Karasu, F.; Croutxé-Barghorn, C.; Allonas, X.; Lecompère, M.; Riess, G.; Zhang, Y.; Esteves, A. C. C.; van der Ven, L. G. J.; van Benthem, R. A. T. M.; de With, G. Highly-interpenetrated and phase-separated UV-cured interpenetrating methacrylate−epoxide polymer networks: Influence of the composition on properties and microstructure. *Mater. Today Commun.* **2016**, *6*, 17−27.

(9) Ligon, S. C.; Liska, R.; Stampfl, J.; Gurr, M.; Mülhaupt, R. Polymers for 3D Printing and Customized Additive Manufacturing. *Chem. Rev.* **2017**, *117*, 10212−10290.

(10) Gebhardt, A.; Hötter, J. S. *Additive Manufacturing: 3D Printing for Prototyping and Manufacturing*; Carl Hanser Verlag GmbH & Company KG, 2016.

(11) Bagheri, A.; Jin, J. Photopolymerization in 3D Printing. *ACS Appl. Polym. Mater.* **2019**, *1*, 593−611.

(12) Decker, C.; Moussa, K. Kinetic study of the cationic photopolymerization of epoxy monomers. *J. Polym. Sci., Part A: Polym. Chem.* **1990**, *28*, 3429−3443.

(13) Salmoria, G. V.; Ahrens, C. H.; Beal, V. E.; Pires, A. T. N.; Soldi, V. Evaluation of post-curing and laser manufacturing parameters on the properties of SOMOS 7110 photosensitive resin used in stereolithography. *Materials Design* **2009**, *30*, 758−763.

(14) Zhao, T.; Li, X.; Yu, R.; Zhang, Y.; Yang, X.; Zhao, X.; Wang, L.; Huang, W. Silicone−Epoxy-Based Hybrid Photopolymers for 3D Printing. *Macromol. Chem. Phys.* **2018**, *219*, 1700530.

(15) Huang, B.; Du, Z.; Yong, T.; Han, W. Preparation of a novel hybrid type photosensitive resin for stereolithography in 3D printing and testing on the accuracy of the fabricated parts. *J. Wuhan Univ. Technol., Mater. Sci. Ed.* **2017**, *32*, 726−732.

(16) Bassett, A. W.; Honnig, A. E.; La Scala, J. J.; Stanzione, J. F., III Network toughening of additively manufactured, high glass transition temperature materials via sequentially cured, interpenetrating polymers. *Polym. Int.* **2021**, *70*, 749−758.

(17) Kuang, X.; Zhao, Z.; Chen, K.; Fang, D.; Kang, G.; Qi, H. J. High-Speed 3D Printing of High-Performance Thermosetting Polymers via Two-Stage Curing. *Macromol. Rapid Commun.* **2018**, *39*, 1700809.

(18) Romeis, M.; Drummer, D. A Dyciandiamine-Based Methacrylate-Epoxy Dual-Cure Blend-System for Stereolithography. *Polymers* **2021**, *13*, 3139.

(19) Auvergne, R.; Caillol, S.; David, G.; Boutevin, B.; Pascault, J.-P. Biobased Thermosetting Epoxy: Present and Future. *Chem. Rev.* **2014**, *114*, 1082−1115.

(20) Erhard, G. *Designing with Plastics*; Carl Hanser Verlag: Munich, 2006; pp 34−38.

(21) Tullo, A. New route planned to biobased ethylene glycol. *Chem. Eng. News* **2017**, *95*, 10.

(22) Puskas, J. E.; Sen, M. Y.; Kasper, J. R. Green polymer chemistry: Telechelic poly(ethylene glycol)s via enzymatic catalysis. *J. Polym. Sci., Part A: Polym. Chem.* **2008**, *46*, 3024−3028.

(23) Fang, C.; Zhu, X.; Cao, Y.; Xu, X.; Wang, S.; Dong, X. Toward replacement of methyl methacrylate by sustainable bio-based isobornyl methacrylate in latex pressure sensitive adhesive. *Int. J. Adhes. Adhes.* **2020**, *100*, 102623.

(24) Le Nôtre, J.; Witte-van Dijk, S. C. M.; van Haveren, J.; Scott, E. L.; Sanders, J. P. M. Synthesis of Bio-Based Methacrylic Acid by Decarboxylation of Itaconic Acid and Citric Acid Catalyzed by Solid Transition-Metal Catalysts. *ChemSusChem* **2014**, *7*, 2712−2720.
(25) Mattar, N.; de Anda, A. R.; Vahabi, H.; Renard, E.; Langlois, V. Resorcinol-Based Epoxy Resins Hardened with Limonene and Eugenol Derivatives: From the Synthesis of Renewable Diamines to the Mechanical Properties of Biobased Thermosets. *ACS Sustainable Chem. Eng.* **2020**, *8*, 13064−13075.
(26) Gioia, C.; Banella, M. B.; Vannini, M.; Celli, A.; Colonna, M.; Caretti, D. Resorcinol: A potentially bio-based building block for the preparation of sustainable polyesters. *Eur. Polym. J.* **2015**, *73*, 38−49.
(27) Nouailhas, H.; Aouf, C.; Le Guerneve, C.; Caillol, S.; Boutevin, B.; Fulcrand, H. Synthesis and properties of biobased epoxy resins. part 1. Glycidylation of flavonoids by epichlorohydrin. *J. Polym. Sci., Part A: Polym. Chem.* **2011**, *49*, 2261−2270.
(28) Aouf, C.; Le Guernevé, C.; Caillol, S.; Fulcrand, H. Study of the O-glycidylation of natural phenolic compounds. The relationship between the phenolic structure and the reaction mechanism. *Tetrahedron* **2013**, *69*, 1345−1353.
(29) Ng, F.; Couture, G.; Philippe, C.; Boutevin, B.; Caillol, S. Bio-Based Aromatic Epoxy Monomers for Thermoset Materials. *Molecules* **2017**, *22*, 149.
(30) Bozell, J. J.; Petersen, G. R. Technology development for the production of biobased products from biorefinery carbohydrates—the US Department of Energy's "Top 10" revisited. *Green Chem.* **2010**, *12*, 539−554.
(31) Branciforti, D. S.; Lazzaroni, S.; Milanese, C.; Castiglioni, M.; Auricchio, F.; Pasini, D.; Dondi, D. Visible light 3D printing with epoxidized vegetable oils. *Addit. Manuf.* **2019**, *25*, 317−324.
(32) Fantoni, A.; Koch, T.; Baudis, S.; Liska, R. Synthesis and Characterization of Homogeneous Epoxy Networks: Development of a Sustainable Material Platform Using Epoxy-Alcohol Polyaddition. *ACS Appl. Polym. Mater.* **2023**, *5*, 731−742.
(33) Woelk, H. Stärke als Chemierohstoff—Möglichkeiten und Grenzen. *Starch-Stärke* **1981**, *33*, 397−408.
(34) Gorsche, C.; Harikrishna, R.; Baudis, S.; Knaack, P.; Husar, B.; Laeuger, J.; Hoffmann, H.; Liska, R. Real Time-NIR/MIR-Photorheology: A Versatile Tool for the in Situ Characterization of Photopolymerization Reactions. *Anal. Chem.* **2017**, *89*, 4958−4968.
(35) Stögerer, J.; Baumgartner, S.; Hochwallner, A.; Stampfl, J. Bio-Inspired Toughening of Composites in 3D-Printing. *Materials* **2020**, *13*, 4714.
(36) Fiore, G. L.; Klinkenberg, J. L.; Pfister, A.; Fraser, C. L. Iron Tris(bipyridine) PEG Hydrogels with Covalent and Metal Coordinate Cross-Links. *Biomacromolecules* **2009**, *10*, 128−133.
(37) Pu, Y.; Cao, S.; Ragauskas, A. J. Application of quantitative 31P NMR in biomass lignin and biofuel precursors characterization. *Energy Environ. Sci.* **2011**, *4*, 3154−3166.
(38) Szczepanski, C. R.; Pfeifer, C. S.; Stansbury, J. W. A new approach to network heterogeneity: Polymerization induced phase separation in photo-initiated, free-radical methacrylic systems. *Polymer* **2012**, *53*, 4694−4701.
(39) Gorsche, C.; Seidler, K.; Knaack, P.; Dorfinger, P.; Koch, T.; Stampfl, J.; Moszner, N.; Liska, R. Rapid formation of regulated methacrylate networks yielding tough materials for lithography-based 3D printing. *Polym. Chem.* **2016**, *7*, 2009−2014.
(40) Barton, J. M. The application of differential scanning calorimetry (DSC) to the study of epoxy resin curing reactions. *Epoxy Resins and Composites I*; Springer: Berlin, Heidelberg, 1985; pp 111−154.
(41) Rozenberg, B. A. Kinetics, thermodynamics and mechanism of reactions of epoxy oligomers with amines. *Epoxy Resins and Composites II*; Dušek, K., Ed.; Springer: Berlin, Heidelberg, 1986; pp 113−165.
(42) Dell'Erba, I. E.; Williams, R. J. J. Homopolymerization of epoxy monomers initiated by 4-(dimethylamino)pyridine. *Polym. Eng. Sci.* **2006**, *46*, 351−359.
(43) Klute, C. H.; Viehmann, W. Heat of polymerization of phenyl glycidyl ether and of an epoxy resin. *J. Appl. Polym. Sci.* **1961**, *5*, 86−95.
(44) Brandrup, J. *Polymer Handbook*, 4th ed.; Wiley & Sons: New York, 1999.
(45) Stanzione, J. F.; Strawhecker, K. E.; Wool, R. P. Observing the twinkling fractal nature of the glass transition. *J. Non-Cryst. Solids* **2011**, *357*, 311−319.
(46) Farooq, U.; Teuwen, J.; Dransfeld, C. Toughening of Epoxy Systems with Interpenetrating Polymer Network (IPN): A Review. *Polymers* **2020**, *12*, 1908.
(47) Hasa, E.; Scholte, J. P.; Jessop, J. L. P.; Stansbury, J. W.; Guymon, C. A. Kinetically Controlled Photoinduced Phase Separation for Hybrid Radical/Cationic Systems. *Macromolecules* **2019**, *52*, 2975−2986.
(48) de Brito, M.; Allonas, X.; Croutxé-Barghorn, C.; Palmieri, M.; Dietlin, C.; Agarwal, S.; Lellinger, D.; Alig, I. Kinetic study of photoinduced quasi-simultaneous interpenetrating polymer networks. *Prog. Org. Coat.* **2012**, *73*, 186−193.
(49) Krzeminski, M.; Molinari, M.; Defoort, B.; Coqueret, X. Nanoscale heterogeneities in radiation-cured diacrylate networks: Weakness or asset? *Radiat. Phys. Chem.* **2013**, *84*, 79−84.
(50) Ye, D.; Chang, C.; Zhang, L. High-Strength and Tough Cellulose Hydrogels Chemically Dual Cross-Linked by Using Low- and High-Molecular-Weight Cross-Linkers. *Biomacromolecules* **2019**, *20*, 1989−1995.
(51) Wagoner Johnson, A. J.; Herschler, B. A. A review of the mechanical behavior of CaP and CaP/polymer composites for applications in bone replacement and repair. *Acta Biomater.* **2011**, *7*, 16−30.
(52) Brostow, W.; Hagg Lobland, H. E.; Khoja, S. Brittleness and toughness of polymers and other materials. *Mater. Lett.* **2015**, *159*, 478−480.
(53) Pfaffinger, M. Hot Lithography − New Possibilities in Polymer 3D Printing. *Laser Tech. J.* **2018**, *13*, 99−101.

https://doi.org/10.1021/acssuschemeng.3c02194
ACS Sustainable Chem. Eng. 2023, 11, 12004−12013